
# QUANTIFYING BEARING FAULT SEVERITY USING TIME SYNCHRONOUS AVERAGING JERK ENERGY

[1]Mohamed AA. Ismail, [2]Nader Sawalhi and [1]Thu-Hien Pham

*[1] DLR (German Aerospace Center), Institute of flight systems, 38108 Braunschweig, Germany.*

*e-mail: Mohamed.Ismail@dlr.de*

*[2]PM University, Al-Khober, KSA.*

Flight control surfaces have the crucial task of allowing the pilot to control the aircraft. Currently, these are generally controlled by hydraulic actuators. As a part of More Electric Aircraft (MAE) trend, some redundant hydraulic actuators are being partially replaced by Electromechanical Actuators (EMA). In order to ensure the ultimate safety of EMA, reliable vibration-based diagnosis capabilities are potentially needed to minimize the catastrophic risk of EMA failure initiated by critical sub-components such as rolling-element bearing. In this paper a new technique to estimate the fault severity of a defective bearing is presented. The technique is based on analyzing the jerk energy gradient of the synchronously averaged fault impact. The averaged signal is extracted by using time synchronous averaging (TSA) triggered by the fault race frequency (FRF) for the detection task and triggered by shaft speed for the quantifying task. FRF is defined, in this work, as the bearing fault frequency of interest divided by the number of rolling elements, which eventually denotes the cage frequency in the case of an outer race fault and the difference between the shaft speed and the cage frequency in the case of an inner race fault. Detailed monitoring of the TSA-based energy is developed for the EMA bearings noting in particular that this can be utilized in other low-speed applications. The effectiveness of the proposed technique is demonstrated and discussed on several seeded faults.

## 1. Introduction

Recently the concept of More-Electric Aircraft (MEA) has gained in popularity throughout several publications, research projects, and prototypes [1, 2]. Integrating electromechanical actuators (EMA) for flight control surfaces realizes MEA strategy. A main technology barrier to incorporate EMA originated from inherent limited reliability as compared with hydraulic actuators. EMA has several sub-components (i.e. bearings, gears, and ball screw) with interfering mechanical contacts that increase the possibility of initiating fatigue cracks and actuator jamming [2].

The main objective of this paper is to investigate an automated vibration-based severity assessment technique that permits to monitor a seeded spall fault in EMA rolling-element bearing. There are two main types of bearing faults; distributed and localized faults. The detection and diagnosis of localized faults at a very early stage is crucial for ensuring reliable operations. Reliable diagnosis

and a trustworthy condition indicator (CI) to measure the equipment severity are the ultimate goals of different fault diagnosis schemes. Due to the criticality of the considered aerospace components, not only the detection of the fault is vital but attention should also be paid to the quantification of the fault in order to realistically track fault progression and establish warning limits. Prognosis analysis needs a fault sensitive CI to produce reliable remaining useful life (RUL) estimation.

Several studies [3-7] presented several characteristics that CI should have, such as monotonic trend, high sensitivity and incorporating statistical confidence. Developing a severity index which satisfies all mentioned requirements is a difficult task. For example, the vibration energy (root mean squared (rms) of a faulty bearing mostly achieves the monotonic behavior however a consistent sensitivity is hard to obtain.

Randall [4] has categorized the state–of-the-art research work on vibration-based diagnosis into three parts: signal separation, enhancement and envelope analysis. The separation process relies on advanced signal processing techniques to isolate bearing vibration signatures from overall vibrations by using adaptive noise cancellation (ANC), discrete/random separation (DRS) or time synchronous averaging (TSA). For complex assemblies, the transmission path may mask the fault signature by shifting dominant resonant frequency and therefore additional enhancement processing is essential. Wavelet denoising and spectral kurtosis are an effective way to enhance the fault frequency band. The envelope analysis embraces several features to quantify fault existence and severity.

Camci [5] evaluates the quality of several vibration features to fulfil bearing prognosis requirements. A fault separation metric was proposed for twelve statistical features such as rms, kurtosis, crest factor and standard deviation for different frequency bands. Standard deviation and rms partially satisfy monotonic property but with limited unsmooth sensitivity.

The paper is organized as follows. In Section 2, the current fault signature theories are briefly compared. In Section 3, bearing testrig and seeded fault geometry are described. Section 4 derives theoretically the energy gradient technique. Finally, Section 5 discusses and experimentally validates the efficiency of the proposed technique.

## 2. Fault Signature Theories

Vibration signature handling from a bearing with localized fault may be mainly performed for two objectives; fault diagnosis and size quantifying. Fault diagnosis focuses on detecting the cyclostationary characteristics associated with the passage of the rolling element over the considered fault. The fault location could be identified by matching the measured impact frequency, using the well-establish envelope analysis technique with one of fault characteristic frequencies; ball pass frequency inner (BPFI) for a fault on the inner race, ball pass frequency outer (BPFO) for a fault on the outer race or ball spin frequency BSF for a fault on the rolling element [3].

For fault size quantification, the time domain signal features associated with the passage of the rolling element over the spalled region should be further analyzed. Several studies have been conducted to describe vibrational features that are correlated with fault size [7-9]. These studies agree on the fact that two main parts of the vibration response should be distinguished; the entry and the exit. The fault size could be measured by the separation (in samples) between rolling element entry point into the fault zone and the impact point.

The earlier theory by Dowling [7] explains the spacing between two high-frequency impulses as a symptom to the entry and exit points as shown in Fig. 1 (left). Dowling interpretations could not be observed for other data. An in depth study by Epps and McCallion [8] shows different behaviors for the entry and the exit. The entry into the fault part comprises gradual de-stress mainly dominated by low-frequency content. The exit part starts when the rolling element instantaneously departures the fault zone and causes sudden change in the direction and high-frequency impulse as shown in the right plot in Fig. 1.

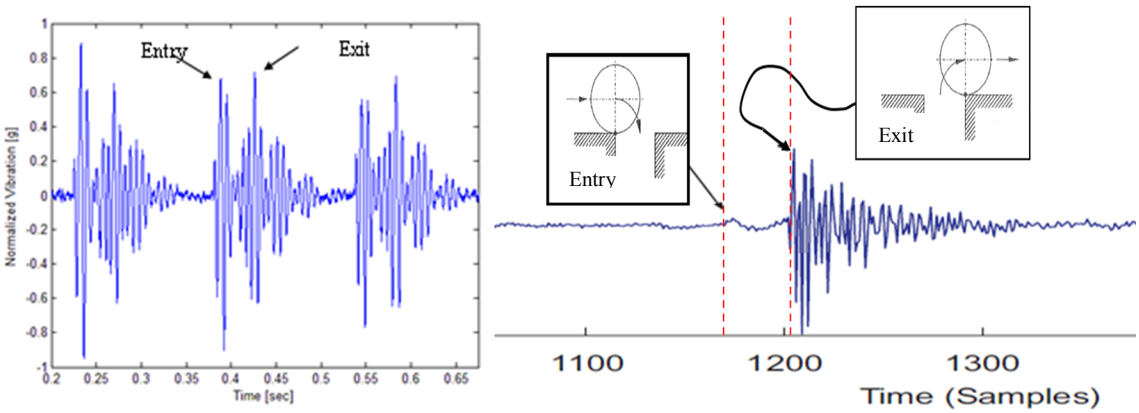


**Fig. 1:** Entry/exit vibrational events at bearing spall edges for 500 rpm (right) and 60 rpm (left).

The low-frequency content of the weak entry event makes it very hard to identify from background noise. The envelope analysis [3], which is the most common vibration based-diagnosis technique, detects the impulse response resulting from the high-frequency impact events and thus the possibility of identifying the actual fault size or severity level diminishes.

Recently, Sawalhi [9] presents two methods to enhance entry part through intensive signal processing schemes namely; joint treatment and separate treatment. The joint treatment utilizes pre-whitening and wavelet analysis to highlight both entry and exit events. On the other hand separate treatment uses a threshold to isolate respectively low-frequency and high-frequency events into two separate envelops with statistical evaluation.

The technique that is proposed in this paper is founded on the entry/exit theory presented by Epps and Sawalhi [8, 9]. The main new idea is that the identification of the entry/exit events is based on the vibrational jerk instead of the vibrational acceleration. The jerk signal has to be extracted by an optimized differentiator to robustly suppress background noise and manifest entry and exit events.

## 3. Description of Seeded Faults and Testrig

The arrangement of the data sets tailors four operating conditions for every fault was set as follows; two speeds (500 and 60 rpm) and two loads (5 kN and 8.8 kN). Three high sensitive accelerometers (model PCB 356A32) were used to measure axial vibrations with sampling frequency of 25.6 kHz and a duration of 30 seconds. In order to perform high resolution angular resampling, quadrature optical encoder with 300 pulses per revolution was used to measure instantaneous angular position instead of using tacho-generator with limited resolution.

Table 1 provides the dimensions of seeded inner and outer race faults introduced into bearing (FAG QJ212TVP), which is a four point's ball bearing that fulfils aerospace requirements for flight control surface EMA. Each fault was seeded by means of a milling tool which forms an oval geometry defined by fault depth and two diameters; the minimum diameter (D1) represents the spall length and maximum diameter (D1) which is perpendicular to the rolling-element track as shown in Fig. 2.

**Table 1**: Seeded faults dimensitions.

| Inner Race Faults | | | | Outer Race Faults | | | |
|---|---|---|---|---|---|---|---|
| Code | Depth [mm] | D1 [mm] | D2 [mm] | Code | Depth [mm] | D1 [mm] | D2 [mm] |
| 0001 | 0.05 | 1.6 | 2.6 | 0100 | 0.05 | 1.4 | 2.6 |
| 0003 | 0.15 | 2.7 | 4.4 | 0300 | 0.15 | 2.4 | 4.4 |
| 0007 | 0.40 | 4.4 | 6.8 | 0700 | 0.40 | 4.0 | 6.8 |

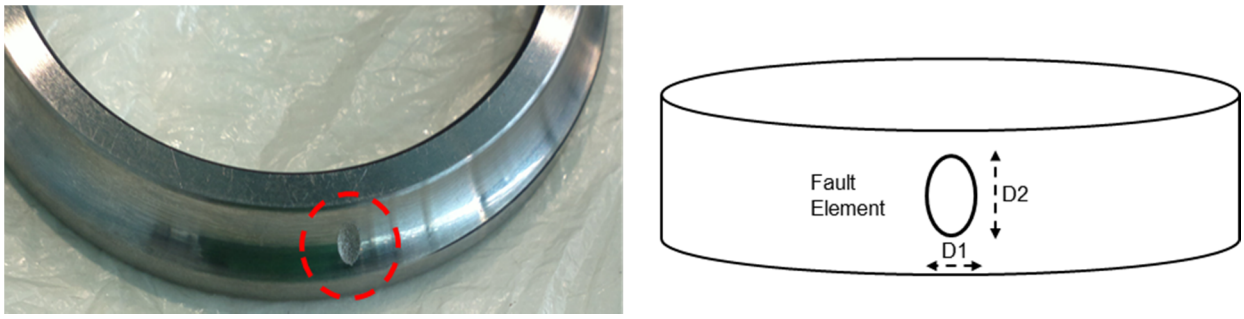


**Fig.2**: Geometry of seeded fault.

## 4. Energy Gradient Technique

According to Section 2, there is a need to set a new treatment to detect entry/exit events which enables more straightforward quantifying of fault size/severity. The energy gradient hypothesis is based on the fact that at both entry and exit points the acceleration is being excited and re-excited respectively. This may be explained in terms of energy balance, the entry edge initiates the vibration which naturally attenuates by structural damping. At the exit edge, a new impact excites the vibration response which suddenly changes the energy rate from decaying into strengthening. Consequently, the proposed technique to detect those points is by deriving (gradient) the acceleration signal and considers only the highest two peaks as a possible entry/exit candidates. The fault severity is then defined by the number of samples between those two peaks. The derivation transforms the acceleration in to a new physical quantity (vibrational jerk) which experimentally establishes more convenient results particularly for low speed applications.

To realize this concept, three steps should be addressed: the separation of non-bearing faults, the robustification of noisy data derivative computation and the statistical analysis of the estimated severity.

*Step 1: Fault Race Frequency (FRF) -Time Synchronous Average (TSA)*

The synchronous average *y(t)* of a time signal *x(t)* using a signal *c(t)* having a trigger frequency ($f_t = 1/T$) is equivalent to the time convolution [3]:

(1) $$y(t) = c(t) * x(t), \quad c(t) = \frac{1}{N}\sum_{n=0}^{N-1}\delta(t+nT)$$

Where *c(t)* is a train of N Dirac delta function spaced by the frequency *1/T*. *x(t)* is kept for vibration signal. The value of *T* governs the performance of TSA. As initial filtering step, by setting *1/T* equal to the shaft speed, the synchronized output y(t) maintains only deterministic vibrations that are synchronized with shaft speed such as unbalance and gears. The bearing vibration could be extracted by:

(2) $$r(t) = x(t) - y(t)$$

Where *r(t)* denotes residual signal which separates all shaft synchronous components such as unbalance and gears *y(t)* from overall vibration *x(t)* , more details in [3, 9].

The detection of the fault frequency using TSA equation is a new contribution in the current work. The fault frequency has a broad spectrum similar to that from a white noise. Setting the TSA trigger frequency as the fault race frequency (FRF) can be used as a tool to check the periodicity of certain fault frequency and associated harmonics. The FRF frequency represents a complete passage of all the rolling elements over the fault and thus comprises all variations on the bearing races. The methodology of new TSA_FRF comprises two stages. The first stage consists in computing the FRF for inner race fault or outer race fault by dividing BPFI or BPFO by the number of balls (nballs).

Due to slip and variable loading, the FRF is converted to a vector composed of 1000 values (0.01% step) lying within ±5% of the nominal FRF value, Eq. (3).

(3) $$T_{FRF} = \frac{1}{[-0.05:0.05]*FRF}, \quad FRF = \frac{BPFI}{nballs} \; or \frac{BPFO}{nballs}$$

The second stage involves substituting each point of $T_{FRF}$ vector in TSA Eq. (1) as a possible trigger frequency. TSA_FRF is the root-mean-squared energy (rms) of y_FRF vector Eq. (4), and used to score different fault frequencies within FRF vector to check fault existence (by comparing faulty/healthy patterns) and to precisely estimate fault frequency which has highest TSA_FRF score.

(4) $$y\_FRF(t,m) = ([\frac{1}{N}\sum_{n=0}^{N-1}\delta(t+nT_{FRF}]*r(t)), \quad TSA\_FRF(m) = \sqrt{\frac{1}{N}\sum_{N} y\_FRF(t)^2}$$

Fig. 3 illustrates the experimental results of estimating TSA_FRF for healthy and faulty bearing. The x-axis refers to fault frequency span under test (±5% fault frequency), while the y-axis denotes to the corresponding normalized TSA_FRF. A significant single sharp peak is only observed for faulty bearing. The ratio of the peak to the mean is used to represent the probability of detected fault frequency.

The main benefits of TSA-FRF are to confirm a certain fault as well as obtaining a very precise estimation of fault frequency for next fault quantifying analysis.

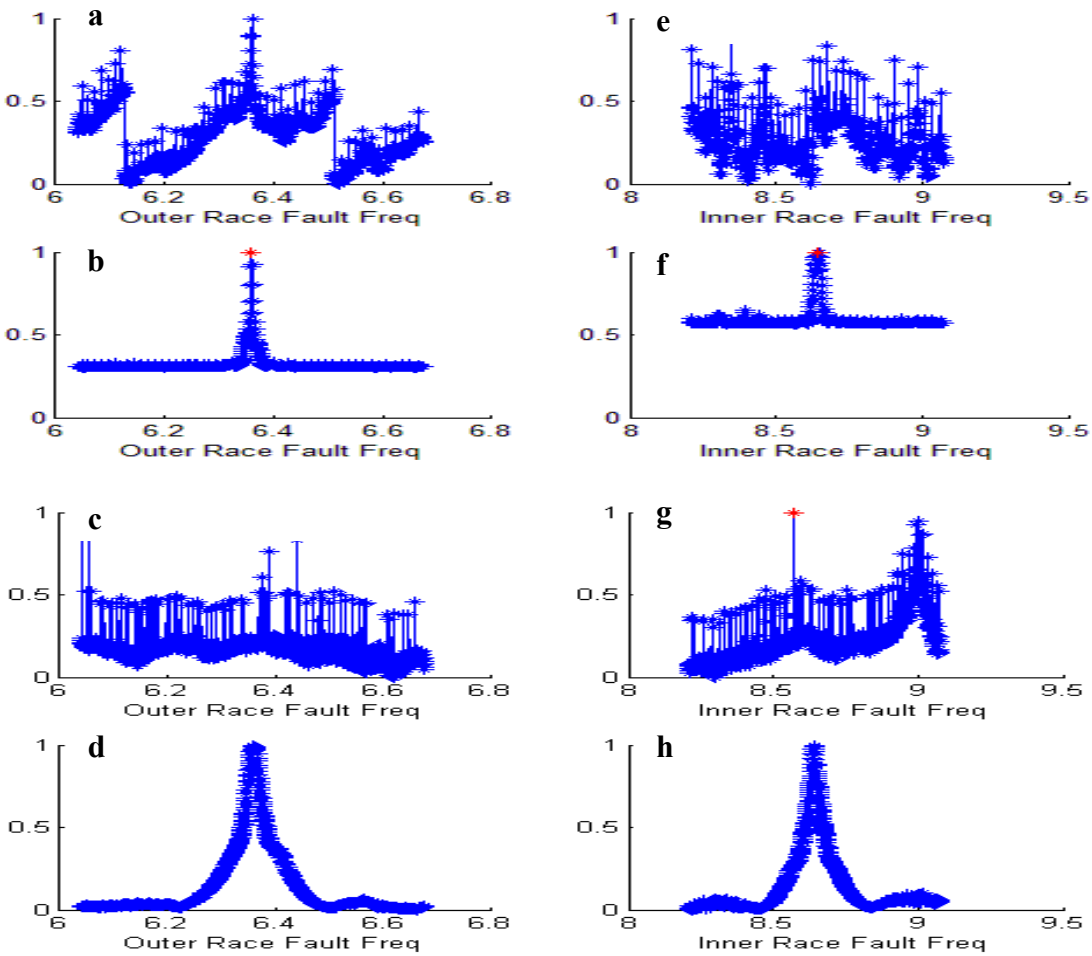


**Fig. 3:** Normalized TSA-FRF for healthy bearing (a, c, e, g) and faulty bearing (b, d, f, h). The upper four plots are in 500 rpm speed and the rest is in 60 rpm.

*Step 2: Noise Robust Differentiator*

The challenge of getting the derivative of extremely noisy vibration data is addressed in this step and is crucial for the success of the energy gradient technique. This has been investigated using well-known algorithms such as Savitzky-Golay filters and spline interpolation. The most satisfactory results were obtained by adapting a smooth noise-robust differentiator developed by Holoborodko [10] in the following formulation:

$$r'_j = \frac{1}{h}\sum_{k=0}^{M} c_k (r_{j+k} - r_{j-k}), \tag{5}$$

$$c_k = \frac{1}{2^{2m+1}}\left[\binom{2m}{m-k+1} - \binom{2m}{m-k-1}\right],\ m = \frac{Nf-3}{2},\ M = \frac{Nf-1}{2} \tag{6}$$

where $r_j$ is the residual vibration for each sample $j$, $h$ represents the sampling time, $Nf$ denotes the filter order and $C_k$ describes the $k$-th filter coefficient. The most critical factor to optimize such filters is the proper estimation of $Nf$ to overcome any changes in background noise, resonant frequency, or sampling frequency. Without an optimal selection of $Nf$, the filter may amplify the noise and smear the fault size features. Therefore all possible values of $Nf$ are analyzed and the best candidate is then selected based on direct searching technique. This optimal value is such that the noise disturbance and the standard deviation of the estimated energy gradient are minimized. Detailed steps of the differentiator filter optimization will be discussed in a separate publication. The energy gradient $\acute{r}_q$ within every fault impact q is the number of samples between the highest two differentiations.

*Step 3: Statistical Processing*

The physical impact between rolling element and the fault is a stochastic process due to several random effects such as ball slippage, lubrication and surface roughness. The measured energy gradient may be considered as a random variable that follows a normal distribution .The first statistical process is applied to detect and remove any possible outliers that have a value significantly greater than population variance. The modified z-score developed by Iglewicz [11] has been used to check for possible outliers:

$$M_q = \frac{0.6745(r'_q - \hat{r}_q)}{median(|r'_q - \hat{r}_q|)} \tag{7}$$

where $r_q$ denotes the energy peaks (i.e. peaks separation) estimated for every fault impact q and $\tilde{r}_q$ denotes the overall median. According to [11], an absolute value of $M_q$ greater than 3.5 is categorized as potential outliers and ignored.

## 5. Results and Discussion

The experimental validation of the proposed technique is based on four vibrational acceleration features. Time kurtosis, crest factor, vibration energy (rms) and spectral kurtosis [3-5] are commonly used statistical features for rolling-element bearing faults. Spectral kurtosis is the current state of the art frequency domain technique to diagnose bearing faults by estimating maximum kurtosis of the optimal frequency band defined by fast kurtogram [12].

The processing of each data set includes using angular resampling to eliminate speed fluctuations as a first pre-processing step. After confirming the fault existence by TSA-FRF technique, a precise estimation of the fault frequency is obtained to separate the peaks for each single fault impact as successive windows have a width of (1/fault frequency) as shown in Fig. 4.a.

The next step is to utilize the robust differentiator to extract the gradient. A filter order of 51 samples has been found to be the best trade-off between vibration gradient separation/identification

and non-amplification of the background noise. As depicted in Fig. 4.b, the fault impacts are transformed to a series of peaks which refer to the vibrational jerk.

The estimated gradients (Fig. 4.c) are weighted by modified z-score in Eq. (7) and the residuals are plotted by the histogram as Fig. 4.d. Finally a normal distribution is fitted and the mean value is taken as the severity index with associated uncertainty defined by the variance (Fig. 4.e). Figure 5 shows the assessment of different faults sizes by five severity features. The monotonic semi-linear trend is only noticed for the new energy gradient method for all fault sizes, at the two operating speeds and 5 kN load. The same results have been also achieved by 8.8 kN load.

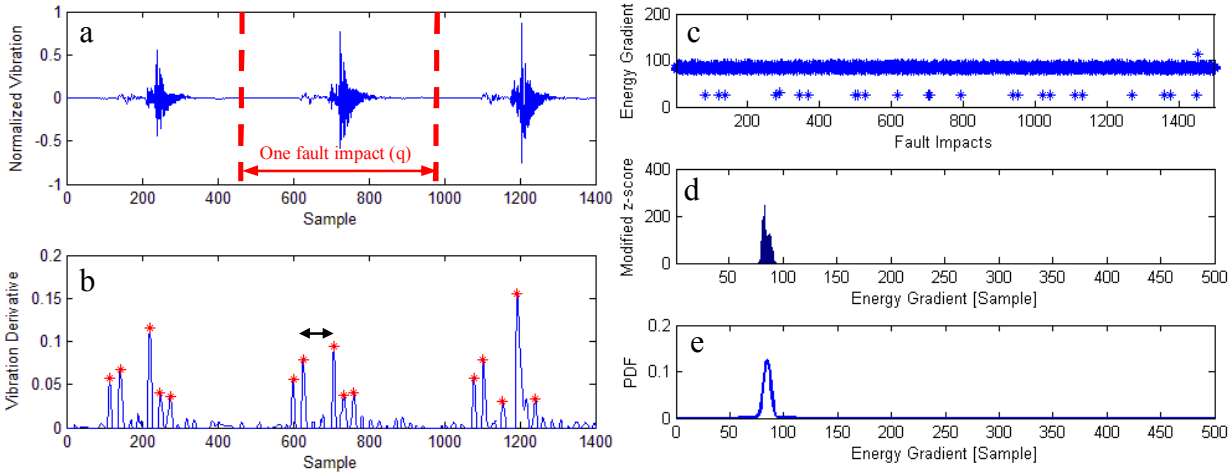


**Fig.4:** (a) Three raw fault impacts (0700, 500 rpm, 5 kN), (b) after applying robust differentiator where the arrow heads refer to the jerk energy gradient of the middle impact, (c) the estimated gradient for 1500 fault impacts, (d) histogram after removing possible outliers, (e) fitted normal probability density function (pdf).

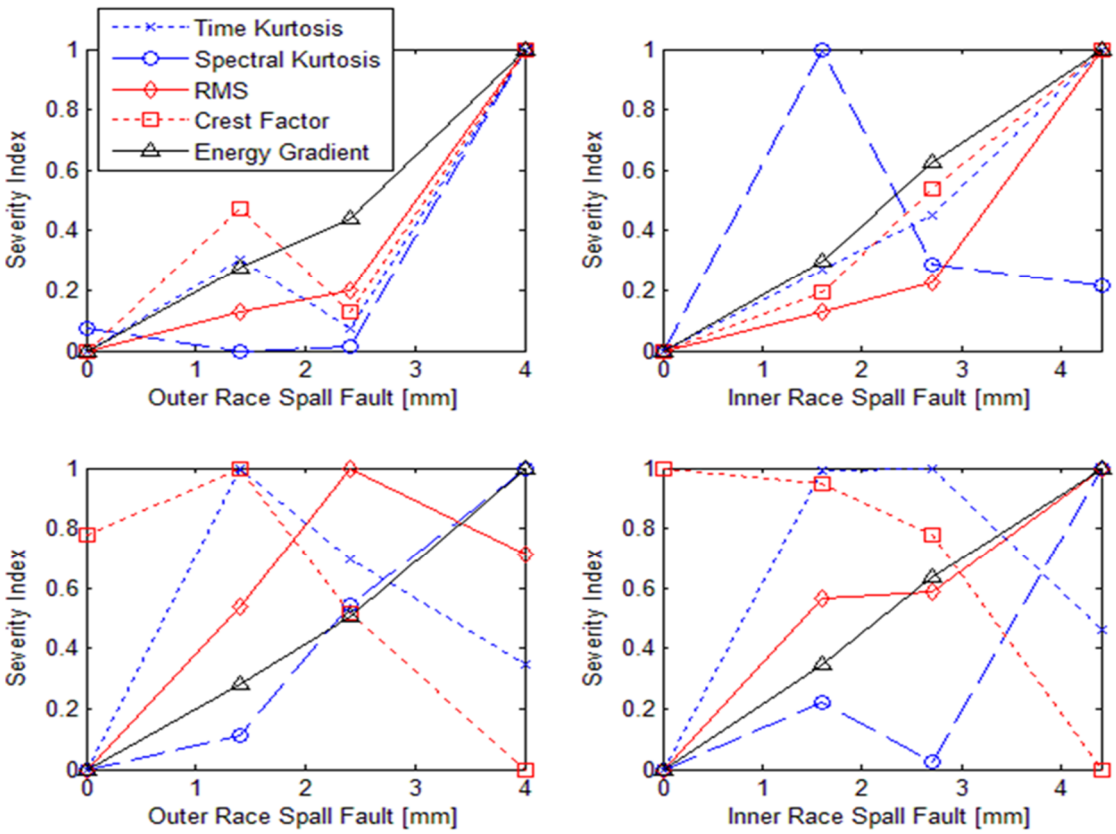


**Fig. 5:** Normalized severity estimated by five features for; 5 kN and 500 rpm (top) and 60 rpm (bottom).

## 6. Conclusion

A novel vibration-based severity index, denoted as the jerk energy gradient, has been proposed and investigated to quantify the bearing spall severity. The proposed method is an automated scheme which includes fault detection as well as statistical quantifying in the time domain. The applicability of using energy gradient as a severity index has been successfully validated for low-speed EMA bearings; 60 and 500 rpm. When compared with several statistical condition monitoring indicators, the proposed severity index was the only one exhibiting a monotonic semi-linear behavior for all fault types and at the different operating conditions. This result supports the chosen approach, which is based on the monitoring of the actual physical events that are triggered by the fault edges. This work presents the groundwork to support the realization of practical prognosis and remaining useful life estimation for many critical applications.

## REFERENCES


1 Janker, P., Claeyssen, F., Grohmann, B., Christmann, M., Lorkowski, T. & LeLetty, R., *New actuators for aircraft and space applications*, The 10th International Conference on New Actuator, Bremen, Germany, June, ( 2006).

2 Balaban, E., Bansal, P., Stoelting, P., Saxena, A., Goebel, K. F., & Curran, S., *A diagnostic approach for electro-mechanical actuators in aerospace systems,* IEEE Aerospace conference, Big Sky, USA, March, (2009).

3 Randall, R. B., *Vibration-based condition monitoring: industrial, aerospace and automotive applications*, John Wiley, ISBN: 978-0-470-74785-8, (2011).

4 Randall, R. B., & Antoni, J., *Rolling element bearing diagnostics*, Mechanical Systems and Signal Processing, 25(2), 485-520, (2010),

5 Camci, F., Medjaher, K., Zerhouni, N., & Nectoux, P., *Feature evaluation for effective bearing prognostics*, Quality and Reliability Engineering International, 29(4), (2013).

6 Rauber, T. W., de Assis Boldt, F., & Varejão, F. M., *Heterogeneous Feature Models and Feature Selection Applied to Bearing Fault Diagnosis*, IEEE Transactions on Industrial Electronics,Vol.62(1), Jan, (2015).

7 Dowling, M., *Application of non-stationary analysis to machinery monitoring*, IEEE International Conference on Acoustics, Speech, and Signal processing, Minneapolis, MN, USA, April, (1993).

8 Epps, I.K. & McCallion, H., *An investigation into the characteristics of vibration excited by discrete faults in rolling element bearings*, Annual Conference of the Vibration Association of New Zealand, Christchurch, New Zealand, (1994).

9 Sawalhi, N., & Randall, R. B., *Vibration response of spalled rolling element bearings: Observations, simulations and signal processing techniques to track the spall size*. Mechanical Systems and Signal Processing, 25(3), 846-870, (2011).

10 Holoborodko, P. (2008), *Smooth noise robust differentiators*.

11 Iglewicz, B. & Hoaglin, D., *How to Detect and Handle Outliers*, ASQC Basic References in Quality Control: Statistical Techniques, (1993).

12 Antoni, J., & Randall, R. B. , *The spectral kurtosis: application to the vibratory surveillance and diagnostics of rotating machines*, Mechanical Systems and Signal Processing, 20(2), 308-331, (2006).